Brain and Spine 4 (2024) 102837

Contents lists available at ScienceDirect

Brain and Spine

journal homepage: www.journals.elsevier.com/brain-and-spine

Embracing uncertainty in cerebrospinal fluid dynamics: A Bayesian approach to analysing infusion studies

Jeremi Chabros [a,*], Michal M. Placek [b,c], Ka Hing Chu [b], Erta Beqiri [b], Peter J. Hutchinson [c], Zofia Czosnyka [b,c], Marek Czosnyka [b,c], Alexis Joannides [c], Peter Smielewski [b]

[a] University of Cambridge School of Clinical Medicine, Cambridge Biomedical Campus, CB2 0SP, Cambridge, UK
[b] Brain Physics Laboratory, Division of Neurosurgery, Department of Clinical Neurosciences, Cambridge Biomedical Campus, CB2 0SP, Cambridge, UK
[c] Department of Neurosurgery, Addenbrooke's Hospital, Cambridge University Hospitals NHS Foundation Trust, CB2 0QQ, Cambridge, UK

ARTICLE INFO

Handling Editor: W Peul

Keywords:
Intracranial pressure
Brain physics
Normal pressure hydrocephalus
Bayesian inference
Cerebrospinal fluid dynamics
Infusion studies

ABSTRACT

Introduction: Cerebrospinal fluid (CSF) infusion test analysis allows recognizing and appropriately evaluating CSF dynamics in the context of normal pressure hydrocephalus (NPH), which is crucial for effective diagnosis and treatment. However, existing methodology possesses drawbacks that may compromise the precision and interpretation of CSF dynamics parameters.
Research question: This study aims to circumvent these constraints by introducing an innovative analysis method grounded in Bayesian inference.
Material and methods: A single-centre retrospective cohort study was conducted on 858 patients who underwent a computerized CSF infusion test between 2004 and 2020. We developed a Bayesian framework-based method for parameter estimation and compared the results to the current, gradient descent-based approach. We evaluated the accuracy and reliability of both methods by analysing erroneous prediction rates and curve fitting errors.
Results: The Bayesian method surpasses the gradient descent approach, reflected in reduced inaccurate prediction rates and an improved goodness of model fit. On whole cohort level both techniques produced comparable results. However, the Bayesian method holds an added advantage by providing uncertainty intervals for each parameter. Sensitivity analysis revealed significance of the CSF production rate parameter and its interplay with other variables. The resistance to CSF outflow demonstrated excellent robustness.
Discussion and conclusion: The proposed Bayesian approach offers a promising solution for improving robustness of CSF dynamics assessment in NPH, based on CSF infusion tests. Additional provision of the uncertainty measure for each diagnostic metric may perhaps help to explain occasional poor diagnostic performance of the test, offering a robust framework for improved understanding and management of NPH.

1. Introduction

1.1. Cerebrospinal fluid dynamics in normal pressure hydrocephalus

Normal Pressure Hydrocephalus (NPH) is a complex neurological disorder characterized by disrupted cerebrospinal fluid (CSF) dynamics, which manifests clinically as the triad of gait instability, dementia, and urinary incontinence (Hakim and Adams, 1965). The elusive nature of this pathology presents an array of diagnostic and therapeutic challenges resulting in a substantial prevalence of underdiagnosis and undertreatment. The consequent implications extend beyond the patient, leading to avoidable healthcare costs and suboptimal clinical outcomes (Lalou et al., 2020).

The current repertoire of diagnostic tools, used to supplement clinical assessment, includes extended lumbar drainage, intracranial pressure monitoring, tap tests, and infusion studies, each presenting its own set of limitations with varying levels of sensitivity and specificity (Thavarajasingam et al., 2021). The primary and most effective treatment modality for NPH is CSF flow diversion via shunt insertion (Hebb and Cusimano, 2001). Yet, it is recognized that the complexity of NPH extends beyond a mere disturbance in CSF circulation (Czosnyka et al., 2021), and individual responses to shunting exhibit significant variability (Lalou et al., 2021). Consequently, the assessment of CSF dynamics has emerged as a crucial factor in making informed decisions

* Corresponding author. Fitzwilliam College, Storey's Way, CB3 0DG, Cambridge, UK.
E-mail address: jjc80@cam.ac.uk (J. Chabros).

https://doi.org/10.1016/j.bas.2024.102837
Received 26 June 2023; Received in revised form 13 May 2024; Accepted 22 May 2024
Available online 22 May 2024
2772-5294/© 2024 The Authors. Published by Elsevier B.V. on behalf of EUROSPINE, the Spine Society of Europe, EANS, the European Association of Neurosurgical Societies. This is an open access article under the CC BY-NC-ND license (http://creativecommons.org/licenses/by-nc-nd/4.0/).

related to prognostication of shunt insertion, diagnosis of shunt malfunction, and proposition of viable solutions when a patient's condition fails to improve post-management.

Infusion studies have proven to offer comprehensive assessment of CSF dynamic parameters. Demonstrating significant diagnostic value in discriminating patients who may benefit from shunting and those for whom the procedure may be unnecessary or possibly even harmful, they form an integral part of the British national best practice guidelines for diagnosing and treating NPH (NICE IPG263). The European iNPH Multicentre Study (Wikkelsø et al., 2013) found that infusion studies show positive predictive value ranging from 86 to 94% for predicting the outcome of shunt treatment in idiopathic NPH patients, while, conversely, they display a contrasting, markedly lower negative predictive value of only 18%. This discrepancy implies a probable under-identification of patients who could potentially benefit from shunting given the current diagnostic criteria. Currently, the selection criteria for patients for shunting rely on a rudimentary thresholding approach, focusing on two parameters of the CSF circulation model: baseline pressure (P_b) and resistance to CSF outflow (R_{out}). Therefore, there is a pressing need for the development of more refined analytical tools to enhance the predictive power of infusion tests. This improvement is crucial for facilitating optimal patient selection, with the aim of maximising the benefits of shunt treatment while minimizing adverse outcomes and associated healthcare expenditures in the management of NPH patients (Lalou et al., 2021).

1.2. Computerised infusion studies

During a CSF infusion study, an additional volume of fluid is introduced at a steady rate into the craniospinal space via either ventricular access (with shunt in situ or preimplanted reservoir) or lumbar access. The consequent intracranial pressure response is measured before, during, and after the infusion (Katzman and Hussey, 1970).

The response to this volume challenge is recorded and traced through the application of a mathematical model of CSF dynamics, initially proposed by Marmarou (Marmarou et al., 1975), and later refined by Avezaat and Eijndhoven (Avezaat and van Eijndhoven, 1984). Although multiple methods of varying complexity have been proposed for the assessment of CSF dynamics, such as the use of multi-compartmental models, constant-pressure infusion test, constant-rate infusion test, or control-theoretic metrics (Linninger et al., 2016), Marmarou model has remained as a model which provides a good balance of simplicity with the amount and type of information it provides. Because the Marmarou model applied to infusion test data has been used in our unit for over 20 years, and owing to our good understanding of the data it produces, we aimed to evaluate the newly-developed method using this model first. The current computerised rendition of this test, originally developed at the Warsaw University of Technology (Czosnyka et al., 1990), is now integrated into the ICM + software for neuromonitoring (Cambridge Enterprise Ltd.) (Smielewski et al., 2009).

The underlying objective of this approach is to identify model parameters that minimise the discrepancy between the pressure response generated by the model and the data collected during the infusion study. Owing to the analytically well-conditioned nature of the model equation and its mathematical tractability, current methods leverage nonlinear gradient descent (GD) algorithms. This methodology is summarised visually in Fig. 1.

1.3. Parameters describing cerebrospinal fluid dynamics

The Marmarou model is characterised by several parameters, among which the resistance to CSF outflow (R_{out}) has received the most attention and is extensively utilised (Czosnyka et al., 2003). R_{out} is a physiological parameter that reflects the ease with which CSF can exit the cranial cavity and enter the venous system. Increased resistance to CSF outflow can cause disruptions in CSF flow, leading to its accumulation, which could potentially result in conditions like hydrocephalus. Various thresholds for the value of this parameter in prognosticating the response to shunting have been suggested, ranging from 12 to 18 mmHg/mL/min (Lalou et al., 2021).

Another variable relevant to the understanding of CSF dynamics is the brain elasticity coefficient (E), also known as the cranio-spinal compliance or elastance factor. It is frequently represented using the pressure-volume index (PVI). This parameter reflects the 'steepness' of the pressure-volume characteristics of the craniospinal spaces. In simpler terms, it describes the rate at which cerebrospinal compliance (the capacity to accommodate volume changes) changes in response to shifts in intracranial pressure. Although a correlation has been observed between this parameter and clinical outcomes related to CSF diversion in obstructive hydrocephalus (Tisell et al., 2002), such results have not been reproduced in the context of NPH (Nabbanja et al., 2018). It is worth noting that this parameter, within the formula for cerebrospinal compliance, is associated with a reference pressure parameter (P_0). While initial assumptions suggested P_0 might represent pressure in the sagittal sinus, these have since been refuted (unpublished results). The physiological significance of this parameter and its impact on the clinical picture in NPH remain unknown, but it is plausible that the interpretation of the elasticity (E) should be considered in conjunction with P_0 (Andersson et al., 2008).

Finally, since hydrocephalus can stem from either a failure of CSF flow or absorption (as reflected by R_{out}) or alterations in the CSF production rate (I_f), the latter parameter itself may hold a prognostic value.

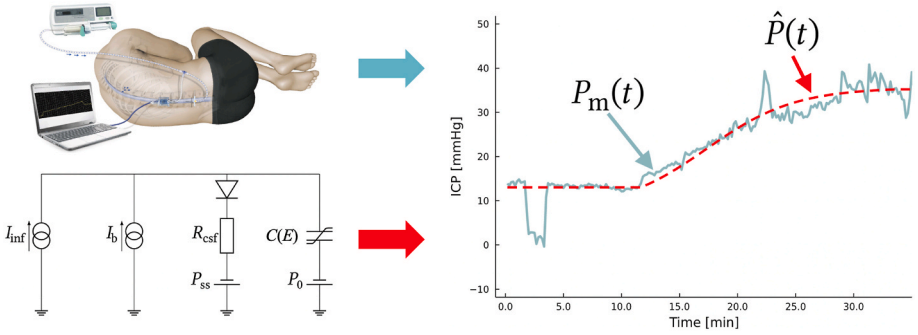

Fig. 1. A diagram showing the curve fitting approach. Data from infusion study (top left) is combined with a model of CSF dynamics (bottom left) and the discrepancy between the two curves can be evaluated (right). P_m is the measured intracranial pressure [mmHg], $\hat{P}(t)$ is the intracranial pressure predicted by the model [mmHg], I_{inf} is the infusion rate [mL/min], I_f is the CSF formation rate [mL/min], R_{out} is the resistance to CSF outflow [mmHg/mL/min], P_{ss} is the pressure in sagittal sinus [mmHg], C is the cerebrospinal compliance [mL/mmHg], and P_0 is the reference pressure [mmHg]. ICP – intracranial pressure.

1.4. Limitations of the current methods

The current methods utilised for estimating cerebrospinal fluid (CSF) dynamics parameters, such as gradient descent (GD)-based optimisation for dynamic fitting and static methods comparing the pressure gradient during infusion, have notable limitations. These shortcomings can broadly be attributed to the model itself, as well as the process of parameter estimation by fitting the model to data.

One primary concern lies in the fact that a perfect mathematical fit achieved using gradient descent methods may not fully represent the physical system it endeavours to model. This can be attributed to factors like measurement noise, artifacts (for example due to patient movement or vascular activity triggered by the infusion), the interdependence of model parameters, their varying sensitivity levels, as well as inherent limitations imposed by the algorithm design.

Moreover, these predictive methods are often agnostic to the physiological context, disregarding the real-world values of these parameters in both patients and healthy controls. This lack of context can lead to potentially erroneous predictions wherein the generated values may fall outside of theoretically plausible ranges (purely because of a better mathematical fit), thereby undermining the clinical relevance and applicability of such predictions.

Further, intrinsic to this model is the fact that some parameters are more sensitive to measurement error than others. However, current techniques fall short in that they only yield point estimates of the CSF dynamics parameters, failing to offer any uncertainty estimates. The absence of confidence intervals for the calculated parameters leaves a gap in our understanding of the potential variability or error associated with these estimates. In clinical settings, where individualised treatment decisions often depend on these parameters, this limitation may present a considerable obstacle in the delivery of optimally personalised care.

Consequently, alternative methods should be sought that not only estimate the CSF model parameters but also assess the uncertainty or errors associated with these estimates. This capability could potentially provide greater confidence in our diagnoses or, conversely, caution when uncertainty is high.

1.5. Aims of the study

Our goal was to address the limitations of parameter estimation by developing a novel Bayesian approach for analysing CSF dynamics using infusion studies. We then sought to validate the performance of this approach using a retrospective database.

2. Methods

2.1. Subjects

We conducted a single-centre retrospective cohort study of 858 patients. The data collection took place at the Cambridge University Hospitals NHS Foundation Trust and the dataset spanned from 2006 to 2020. During this period, these patients underwent specialized computer-aided constant rate infusion tests as part of their clinical investigations for diagnosing NPH. None of the patients involved in the study had a shunt in place at the time of the investigation. Our dataset was fully anonymised and its use for retrospective analysis has been approved by the UK Research Ethics Committee (REC 23/YH/0085).

2.2. Data collection

The protocol for lumbar infusion studies was employed as detailed in prior work by our unit (Czosnyka et al., 2005; Smielewski et al., 2012; Levrini et al., 2021).

The procedure begins with a lumbar puncture, using either one or two 21-gauge Quincke needles positioned under lidocaine local anaesthesia at the L4-L5 intervertebral space with the patient in a lateral decubitus position.

Strict aseptic technique was followed, including cleaning of the skin with an antiseptic solution, and carefully preserving the sterility of the pre-filled tubing and transducer. Our apparatus consisted of a standard, disposable fluid-filled pressure transducer (Edwards Lifesciences™ manometry lines, 180 cm length, 1.2 mm inner diameter) and a pressure amplifier (Spiegelberg or Philips). The high-resolution pressure waveform data was collected with a sampling rate of 30 Hz (earlier years) to 100 Hz (later years) and processed by the ICM + software (Cambridge Enterprise Ltd., Cambridge, UK).

Once acceptable CSF pulse waveform was established, baseline pressure was recorded for 10 min followed by infusion of Hartmann's solution at 1.5 mL/min. If the baseline ICP was above 15 mmHg, the rate was adjusted to 1.0 mL/min. This rate was maintained until a plateau in ICP was observed over a period of 5–10 min. As a safety measure, any surge in mean ICP to 40 mmHg or above necessitated an immediate halt in infusion. The overall duration of the infusion test was approximately between 30 and 45 min.

The conclusion of the infusion test initiated a pressure-controlled withdrawal of CSF via a tap connected to the pressure lines, leaving the pressure transducer in situ. The procedure was halted when the pressure dropped to about 10 mmHg or when the patient reported discomfort such as headache or blurred vision. The raw ICP waveform signal was pre-processed in order to calculate time trends of pulse amplitude AMP (as the Fourier fundamental harmonic of the pulse), and mean ICP, used in further analysis of the pressure response to the CSF infusion. Calculations were performed with data downsampled to 0.1 Hz. Finally, the duration of baseline, plateau ICP recording, the transition phase of rising ICP, and the total infusion time were manually defined upon concluding the infusion test.

2.3. Model specification

We sought to fit the Marmarou model of cerebrospinal fluid (CSF) dynamics to experimental data obtained from CSF infusion studies. Since the values of baseline ICP (P_b) [mmHg] and infusion rate (I_{inf}) [mL/min] are fixed and characteristic to each recording, our model fitting problem can be defined as

$$\widehat{P}(R_{out}, E, P_0, t) = \frac{(I_f + I_{inf}) \times (P_b - P_0)}{I_f + I_{inf} \times \exp(-Et(I_f + I_{inf}))} + I_{inf} \tag{1}$$

$$I_f = \frac{P_b - P_{ss}}{R_{out}} \tag{2}$$

$$P_{ss} \approx P_0 \tag{3}$$

where $\widehat{P}$ is the model pressure [mmHg], R_{out} is the resistance to CSF outflow [mmHg/mL/min], E is the elasticity coefficient [1/mL], t is time [min], P_0 is the reference pressure [mmHg], I_f is the CSF formation rate [mL/min], I_{inf} is the infusion rate [mL/min], and P_b is the baseline pressure [mmHg].

More specifically, we are seeking parameter values that minimise the discrepancy between the ICP trace measured during the infusion study P_m and our model $\widehat{P}$. To evaluate the goodness of fit, we have chosen the residual sum of squares (SSE)

$$\mathrm{SSE}(R_{out}, E, P_0) = \sum_{t=1}^{T} (P_m(t) - \widehat{P}(R_{out}, E, P_0, t))^2 \tag{4}$$

because of its preferential behaviour with the chosen optimisation method. Our objective then takes the form:

$$\widehat{\theta} = \underset{R_{out}, E, P_0}{\mathrm{argmin}} \mathrm{SSE}(R_{out}, E, P_0). \tag{5}$$

2.4. Bayesian optimisation approach

To determine parameter values that best fit the experimental data, while simultaneously accounting for physiological constraints and providing uncertainty measures, we employed a Markov Chain Monte Carlo (MCMC) approach. MCMC is a simulation framework which combines the model with data based on prior beliefs about the distributions of parameter values and arrives at the posterior (i.e. post-experiment) distributions of the estimated parameters following a large number of repeated simulations. The method proves particularly useful in scenarios where the parameter values possess tangible (physiological) significance, and their population level distributions are known or can be heuristically estimated based on expert knowledge. While there are multiple MCMC methods, for the proof-of-concept explorations in the current work, the Metropolis-Hastings (MH) algorithm (Metropolis et al., 1953; Hastings, 1970) was chosen for its simplicity, mathematical tractability, and because this early method is well-understood theoretically and practically, owing to its ubiquity in data sciences and engineering.

The Bayesian method was implemented entirely in Julia (Bezanson et al., 2017). This approach is visually represented in Fig. 2.

The likelihood function, in other words the probability of the data given the parameters, was based on the Gaussian approximation and thus the mean-square error of the model fit to the data.

The prior distributions of the parameters were chosen to be Gaussian, with the mean and standard deviation for each parameter established based on values reported in the literature. These were calculated as weighted averages based on reported values and study sample sizes. We further constrained the search space by imposing either hard or soft (using sigmoid transformation and penalty terms) limits, based on the theoretically permissible ranges for parameter values. For instance, R_{out} cannot be negative, and the elasticity coefficient is a ratio, therefore E must fall within the range of [0, 1]. The prior distributions and ranges are summarised in Table 1.

A more comprehensive model derivation and MCMC specification are presented in the Appendix.

2.5. Method validation

The new Bayesian algorithm was compared against results obtained via the gradient descent (GD) algorithm implemented in ICM + using the following criteria.

1. Rates of erroneous parameter predictions (those outside of pre-defined physiologically permissible ranges as stated in Table 1).
2. Root-mean-square error (RMSE) of the curve fitting.

Table 1
Table summarising the prior knowledge of the parameter distributions and ranges. μ – mean, σ – standard deviation, Min – minimum permissible parameter value, Max – maximum permissible parameter value. R_{out} – resistance to CSF outflow, E – elasticity coefficient, P_0 – reference pressure, I_f – CSF production rate.

Parameter	μ	σ	Min	Max	Study (sample size)
R_{out}	10.45	2.03	0.01	50.00	(Malm et al., 2011) ($n = 40$) (Albeck et al., 1991) ($n = 8$) (Ekstedt, 1978) ($n = 58$) (Albeck et al., 1998) ($n = 52$)
E	0.33	0.08	0.00	1.00	(Szewczykowski et al., 1977) ($n = 10$) (Czosnyka et al., 1988) ($n = 24$) (Wahlin et al., 2010) ($n = 37$) (Okon et al., 2018) ($n = 18$)
P_0	5.21	3.67	−10.00	P_b	(Ekstedt, 1978) ($n = 58$) (Czosnyka et al., 1990) ($n = 43$)
I_f	0.35	0.14	0.01	1.00	(Deck and Potts, 1969) ($n = 16$) (Rubin et al., 1966) ($n = 11$) (Cutler et al., 1968) ($n = 12$) (Masserman, 1934) (n = 284) (Huang et al., 2004) ($n = 23$) (Piechnik et al., 2008) ($n = 12$) (Penn et al., 2011) ($n = 4$) (Gideon et al., 1994) ($n = 18$) (Yoshida et al., 2009) ($n = 6$) (Rottenberg et al., 1977) ($n = 3$) (Silverberg et al., 2001) ($n = 21$) (Lorenzo et al., 1970) ($n = 12$)

3. Coefficient of determination (R^2) of the pressure-volume (P–V) curve.

2.6. Statistical analysis

Based on the normality assessment, appropriate statistical tests were chosen for further analysis. Since the data were found to be non-normally distributed, the nonparametric Wilcoxon signed-rank test for dependent samples was employed for comparisons between the methods.

The significance level (α) was set at 0.05. Effect sizes were calculated using Cliff's delta, a robust and nonparametric measure that estimates the probability that a randomly chosen score from one group will be larger than a randomly chosen score from another group. Cliff's delta values were interpreted as follows: negligible (<0.147), small

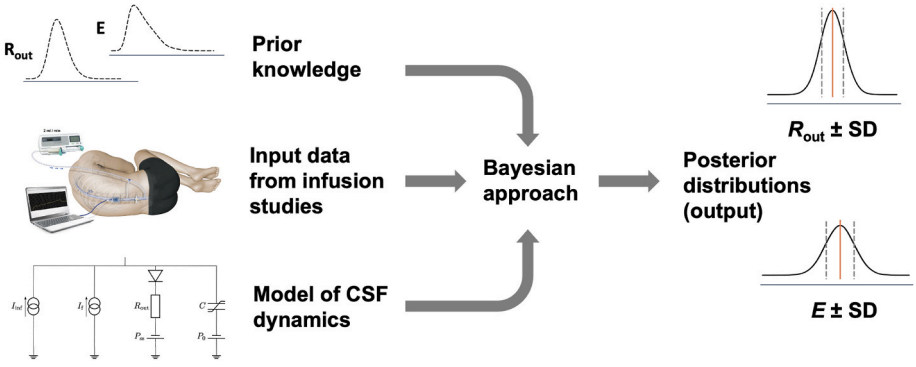

Fig. 2. A schematic representation of the Bayesian approach. Apart from input data and model, this method utilises information about the parameter value distributions. The main advantage is that it produces value distributions instead of point estimates. Therefore, one can evaluate uncertainty (here shown as standard deviation) for each parameter prediction. For simplicity, only two parameters (E, R_{out}) are shown. Posterior ∝ Likelihood × Prior. R_{out} – resistance to CSF outflow, E – elasticity coefficient.

(0.147–0.33), medium (0.33–0.474), and large (>0.474) effect sizes.

The convergence of the MCMC simulations was assessed through both qualitative and quantitative methods. Trace plots and autocorrelation functions (ACF) were used for visual inspection, helping to gauge the stability and mixing properties of the chains. Quantitatively, convergence was assessed using the Gelman-Rubin R statistic (Gelman and Rubin, 1992), derived from triplicate runs for each recording. An $\widehat{R}$ value below 1.3 indicated satisfactory convergence, while $\widehat{R}$ below 1.1 denoted excellent convergence. This multifaceted approach ensured the reliability of the MCMC estimates for the parameters being studied.

The computational analyses were performed on a personal MacBook Air (2020 model) equipped with an Apple M1 chip and 16 GB of RAM, which provided sufficient processing power for the tasks involved. All statistical analyses were carried out in Julia 1.7.3 (Bezanson et al., 2017) using the HypothesisTests.jl package.

3. Results

3.1. The Markov chain-Monte Carlo convergence

Visual examination of the MCMC chain traces did not reveal any signs of correlation among the samples. Furthermore, ACF plots indicated rapid decrease in autocorrelation, suggestive of swift convergence, which was observed in all instances. Therefore, a commonly used empirical burn-in period of 20% of chain length was chosen.

During method development, satisfactory convergence was observed typically between 10^4 and 10^6 iterations. A mark of 10^5 iterations achieved satisfactory convergence for 99% (850/858) and 98% (838/858) of recordings at $\widehat{R}$ below 1.3 and $\widehat{R}$ below 1.1 thresholds, respectively. Computational time for 10^4 iterations was under a second, while 10^5 and 10^6 iterations required 4–7 s and 20–50 s per recording, respectively.

3.2. Parameter value distributions

The median resistance to CSF outflow for the Bayesian method was 12.15 mmHg/mL/min (interquartile range (IQR): 8.80 mmHg/mL/min, 1st quartile(Q1)–3rd quartile (Q3): 8.58–17.39 mmHg/mL/min), while for the gradient descent method it was 12.36 mmHg/mL/min (IQR: 8.54 mmHg/mL/min, Q1–Q3: 8.64–17.18 mmHg/mL/min). The Wilcoxon signed-rank test revealed a significant difference (W = 156237, p < 0.0001), and the effect size, measured using Cliff's delta, was 0.576, indicating a large effect with slightly higher resistance values for the gradient descent method.

The median elasticity coefficient for the Bayesian method was 0.20 mL^{-1} (IQR: 0.24 mL^{-1}, Q1–Q3: 0.11–0.36 mL^{-1}), while for the gradient descent method it was 0.15 mL^{-1} (IQR: 0.15 mL^{-1}, Q1–Q3: 0.10–0.25 mL^{-1}). The Wilcoxon signed-rank test revealed a significant difference ($W = 293318$, $p < 0.0001$), and the effect size, measured using Cliff's delta, was 0.203, indicating a small effect with slightly higher elasticity coefficients for the Bayesian method.

The median CSF production rate for the Bayesian method was 0.39 mL/min (IQR: 0.74 mL/min, Q1–Q3: 0.11–0.85 mL/min), while for the gradient descent method it was 0.48 mL/min (IQR: 0.71, Q1–Q3: 0.28–0.99 mL/min). The Wilcoxon signed-rank test revealed a significant difference ($W = 70762$, $p < 0.0001$), and the effect size, measured using Cliff's delta, was 0.806, indicating a large effect with higher CSF production rates for the gradient descent method.

The median reference pressure for the Bayesian method was 5.63 mmHg (IQR:

9.07 mmHg, Q1–Q3: 0.40–9.47 mmHg), while for the gradient descent method it was 4.91 mmHg (IQR: 9.09 mmHg, Q1–Q3: −0.18–8.91 mmHg). The Wilcoxon signed-rank test revealed a significant difference ($W = 278558$, $p < 0.0001$), and the effect size, measured using Cliff's delta, was 0.243, indicating a small effect with slightly higher reference pressures for the Bayesian method. All histograms showing parameter value distributions are summarised in Fig. 3.

3.3. Fitting error

The errors of the fit were found to not follow normal distributions and therefore the Wilcoxon signed-rank test has been used for comparisons between medians. The median RMSE of the gradient descent method was 0.54 mmHg (IQR: 0.36 mmHg, Q1–Q3: 0.39–0.78 mmHg) and for the Bayesian method it was 0.50 mmHg (IQR: 0.36 mmHg, Q1–Q3: 0.36–0.72 mmHg) which was found to be statistically significant ($W = 23229$, $p < 0.00001$) with a large effect size (Cliff's $\delta = 0.936$).

Because the goodness of fit of the pressure-volume curve has not been used during the optimisation process, it provided an objective measure of method performance. An example comparison for a single patient is shown in Fig. 4.

We compared the coefficient of determination (R^2) of the pressure-volume curve obtained using the two methods: gradient descent and Bayesian. The coefficient of determination for the gradient descent method was 0.77 (IQR: 0.38, Q1–Q3: 0.53 0.91), while for the Bayesian method it was 0.77 (IQR: 0.39, Q1–Q3: 0.52–0.91). The Wilcoxon signed-rank test revealed a significant difference ($W = 156134$, $p = 0.0030$) and the effect size, measured using Cliff's δ, was 0.558, indicating a large effect with higher R^2 values for the gradient descent method. The graphical representation of value distributions is shown in Fig. 5.

3.4. Rates of erroneous predictions

Each CSF dynamics parameter is a value with physiological meaning. Therefore, we evaluated how well both methods accounted for the known constraints of parameter ranges based on previous research.

CSF production rate was the most sensitive parameter, with 211 (24.6%) out-of-range estimates with the gradient descent method, and 15 (1.7%) false predictions with the new method. Resistance to CSF outflow has proven to be the most robust parameter with no false predictions with either method. Elasticity coefficient and reference pressure ranged from 0 (0.0%) to 2 (0.02%) erroneous estimates. The rates of erroneous predictions are summarised in Table 2.

3.5. Uncertainty distributions

The standard deviation (SD) of posterior probability for parameter estimation for elasticity coefficient was found to be 0.02 mL^{-1} (IQR: 0.04 mL^{-1}, Q1-Q3: 0.01–0.05 mL^{-1}). This corresponds to 2% of the physiological range (0.01–1.00 mL^{-1}) for this parameter.

The SD of R_{out} was 0.21 mmHg/mL/min (IQR: 0.31 mmHg/mL/min, Q1-Q3: 0.14–0.45 mmHg/mL/min). This value is equivalent to 0.42% of the physiological range (0.01–50.00 mmHg/mL/min) for this parameter.

The CSF production rate was 0.05 mL/min (IQR: 0.09 mL/min, Q1-Q3: 0.02–0.11 mL/min). This accounts for 5% of the physiological range (0.01–1.00 mL/min) for this parameter. Finally, the reference pressure was 0.73 mmHg (IQR: 1.00 mmHg, Q1-Q3: 0.35–1.35 mmHg). However, since this parameter does not possess a consistent range (the maximum value is dependent on the baseline pressure), it is not feasible to establish a percentage equivalent summary.

The uncertainty distributions for the whole cohort are shown in Fig. 6.

4. Discussion

Accurate assessment and understanding of cerebrospinal fluid CSF dynamics in NPH are crucial for precise diagnosis and effective treatment. This study addresses some of the limitations of current methods by introducing a novel Bayesian approach aimed at refining the prediction of CSF dynamics parameters based on infusion studies. To the best of our

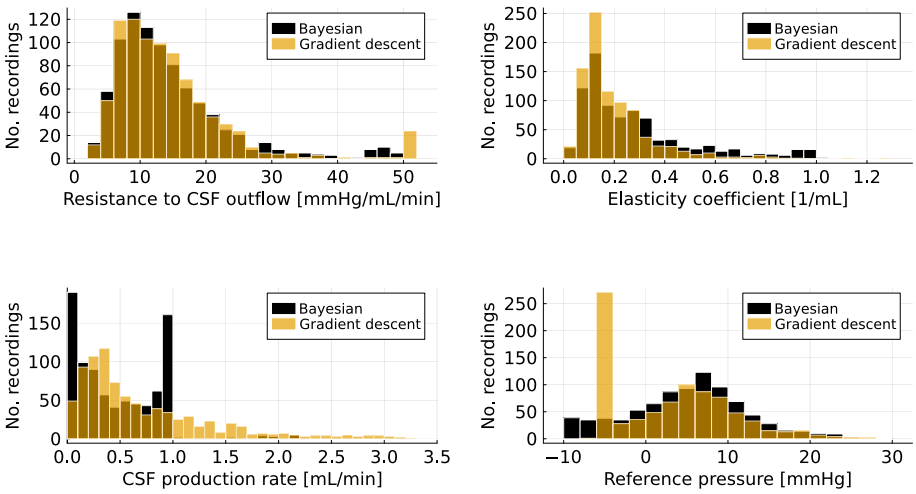

Fig. 3. Histograms showing parameter value distributions for each method. Resistance to CSF outflow (top left), elasticity coefficient (top right), CSF production rate (bottom left), and reference pressure (bottom right). The results from each method have been overlaid. Bayesian method is depicted in solid black, and the gradient descent method is depicted in semi-transparent orange.

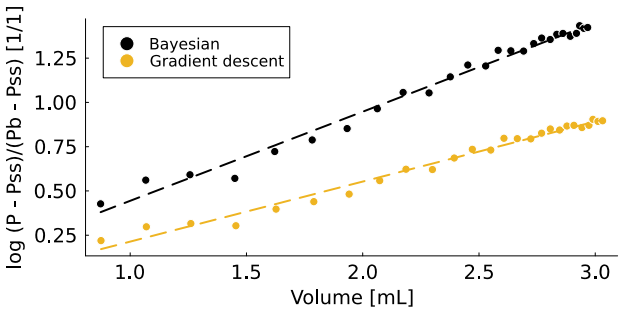

Fig. 4. The figure presents a scatter plot that juxtaposes the pressure-volume curves derived from two distinct methodologies for a single patient, with the y-axis being depicted in a semi-logarithmic scale. In this illustrative instance, the Bayesian method exhibits a coefficient of determination (R^2) of 0.99, while the gradient descent method yields an R^2 value of 0.93. This disparity indicates a marginally superior fit when employing the parameters obtained using the Bayesian approach. It is important to note that the volume represented here does not pertain to the infused fluid volume; rather, it characterizes the change in the volume of the craniospinal space in response to the infusion. P – measured intracranial pressure, Pss – sagittal sinus pressure, Pb – baseline pressure.

knowledge, no prior research has been conducted on a similar topic. Consequently, our efforts focused on comparing the new Bayesian method with the current state-of-the-art gradient descent (GD) method.

The parameter value distributions obtained for the entire cohort using both methods were remarkably similar, which was reassuring. Noteworthy, the Bayesian method returned marginally higher values for elasticity and reference pressure while producing lower values for resistance to CSF outflow and CSF production rate. Except for I_f, the distributions of parameter estimates obtained with both methods displayed substantial overlap. The peaks at the parameter range limits can be attributed to the restrictions enforced by the algorithm design. The noticeable peak at −5 mmHg in P_0 resulted from this value being chosen as the lower limit for the gradient descent method.

A significant limitation of existing methodologies is their potential for erroneous predictions of CSF dynamics parameters. Our results demonstrated that the GD-based optimisation method experienced higher rates of inaccurate predictions compared to our Bayesian approach. Specifically, we noted significantly lower rates of inaccurate predictions for all parameters using the Bayesian method, with the CSF production rate showing the most remarkable improvement. This superiority was expected based on the Bayesian method's design, which inherently incorporates both theoretical and empirical constraints on parameter values, while also incorporating prior knowledge. Therefore, we anticipated that the uncertainty associated with I_f would be higher for the GD method, as it would incorporate variability from R_{out} and P_0, whereas the Bayesian method handles the calculation of non-optimized I_f in a post hoc manner using the values of P_0, R_{out}, and P_b. In line with

Table 2
A table showing the comparison in erroneous prediction rates for the gradient descent (current) and the Bayesian (new) methods. Rout – resistance to CSF outflow, E – elasticity coefficient, P0 – reference pressure, If – CSF production rate.

Parameter	Gradient descent	Bayesian
R_{out}	0 (0%)	0 (0%)
E	2 (0.2%)	0 (0%)
P_0	2 (0.2%)	2 (0.2%)
I_f	211 (24.6%)	15 (1.7%)

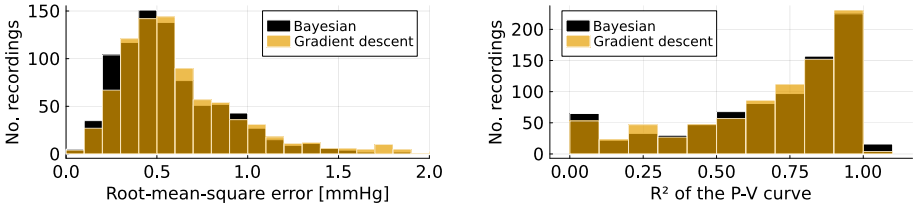

Fig. 5. Histograms showing goodness of fit diagnostics for both methods: Root-mean-square error of the model fit to data (left), and coefficient of determination of the pressure-volume curve (right). The results from each method have been overlaid. Bayesian method is depicted in solid black, and the gradient descent method is depicted in semi-transparent orange.

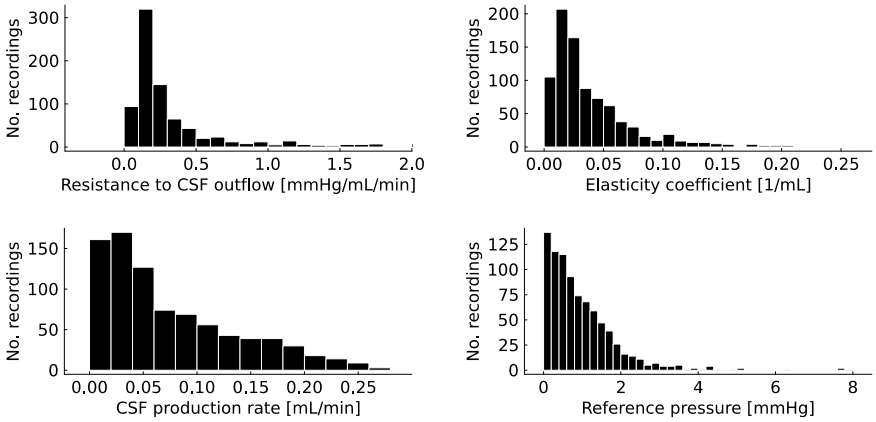

Fig. 6. Histograms showing standard deviations for parameter value distributions for the Bayesian method. Resistance to CSF outflow (top left), elasticity coefficient (top right), CSF production rate (bottom left), and reference pressure (bottom right).

this, the Bayesian method's uncertainty analysis showed that the standard deviation for this parameter equalled 5% of its theoretically admissible physiological range, the highest among all parameters. Conversely, the resistance to CSF outflow demonstrated exceptional robustness, with no erroneous predictions and the lowest uncertainty (0.42%) compared to other parameters.

We also evaluated the fitting error of the two methods. Our findings indicated that the Bayesian approach significantly outperformed the gradient descent method in terms of the root mean-square error (RMSE) of curve fitting. This improvement could be attributed to the fact that the MCMC methods, which form the basis of our Bayesian approach, explore the search space more efficiently and are less prone to issues like local minima, which can affect GD-based methods. While the two methods demonstrated identical median coefficients of determination for the pressure-volume (P–V) curve, the Wilcoxon ranked sum test returned a significant difference between them. Even though the shapes of the error distributions were nearly identical, this finding could be attributed to the fact that the Wilcoxon test is based on ranks of the data rather than the actual data values. Thus, even with identical medians, a significant difference can be detected if the ranks of the data points within each group differ. In conclusion, the goodness of fit achieved by our new Bayesian method was superior to or at least comparable to that of the current gradient descent method.

4.1. Measuring uncertainty

Unlike the traditional gradient descent method, which provides point estimates, our method offers the entire posterior probability distribution, thus incorporating uncertainty into the prediction. This is a significant advantage, and the inclusion of uncertainty measures is crucial in clinical decision-making, as it may enable clinicians to assess the variability and reliability of the estimated parameters and provide a more nuanced understanding of the infusion test results, which can be particularly useful when the results are close to the widely recognized thresholds.

With the gradient descent method, some patients would have been classified as having a positive test result (above the threshold), and some would have been classified as having a negative test result (below the threshold). In contrast, our Bayesian method does not force a binary classification but rather provides a probability distribution of potential outcomes.

To interpret the results from our new method, if both the central tendency (mean or median) and the entire confidence interval (or credible interval in the Bayesian context) fall below or above the threshold, the results can be interpreted similarly to the gradient descent method. However, for cases where the probability distribution crosses the threshold, we propose three potential strategies.

1. Classify these cases as indeterminate, requiring further diagnostic or clinical information for a definitive diagnosis.
2. Use the entire probability distribution and assign the test result based on the side with the greater probability density mass.
3. Report the result as either positive or negative but provide the associated probability that the result is true.

This approach embraces the inherent uncertainty in medical testing and decision-making and may improve the clarity of communication between physicians and patients regarding the likelihood of a particular diagnosis. Future research is needed to determine the optimal strategy for interpreting results that cross the diagnostic threshold and their potential impact on clinical practice, influencing guidance and indications for shunt placement.

4.2. Limitations

Despite the promising findings and novel approach presented in this research, there are several limitations that merit further discussion. First, it is important to stress that the aim of this research was to validate the new approach by comparing it to an existing method, in the absence of a universally accepted gold standard. Reconciling our findings with patient outcome data would improve our capacity to thoroughly compare the predictive power achieved by parameter predictions obtained with each method.

In addition, our new approach relies heavily on the implementation of MCMC methods. These are versatile, capable of handling diverse likelihood functions and parameter distributions. However, their efficiency and convergence are impacted by the choice of priors, particularly in sparse data scenarios. In our study, we bolstered the reliability of the priors by basing them on extensive published data obtained from various patient cohorts using diverse experimental techniques. MCMC approach may be robust to the choice of priors, especially in situations where the quality and amount of data allows the data to dominate the prior in calculating the posterior distribution. This feature arises as result of asymptotic validity, Markov chain property, mixing and adaptation mechanisms. However, the choice of priors can also affect the convergence and the estimates. Therefore, it is important to carefully consider and assess the impact of prior assumptions, especially in cases where the priors might be uncertain or misspecified. For example, the empirical distributions of some of the optimized parameters do not conform to perfect Gaussians. Therefore, a more extensive investigation into the choice of prior distributions and their parameters is warranted in future research.

Moreover, despite their benefits, MCMC methods can be computationally demanding and assessing chain convergence can be complex. In our research, due to the lower dimensionality of our search space and the relative simplicity of our objective function and model, feasible iteration counts for standard computers yielded computation times within seconds. We meticulously evaluated convergence both visually using the autocorrelation function (ACF) and MCMC chain trace plots, and statistically using the well-established Gelman-Rubin statistic.

Finally, while our study benefited from a large patient population, it was not a multicentre trial. The generalizability and external validity of our Bayesian approach would be strengthened through further validation in larger, multicentre studies, which would offer more diverse patient profiles and conditions, reflecting possible differences in data collection and care settings. Thus, in future research, it will be important to secure a dataset inclusive of comprehensive clinical outcome data.

4.3. Clinical relevance and future directions

This work introduces a new Bayesian methodology, focusing on evaluating its feasibility and performance compared to the current GD approach. The results provided herein demonstrate non-inferiority, and potential superiority, of this method across an array of performance metrics. A critical future direction is the assessment of its clinical utility, with the emphasis on the added benefit of uncertainty estimation.

As an example, Wikkelsø et al. (2013) proposed $R_{\text{out}} > 12$ mmHg/mL/min as the only parameter to show prognostic utility in the evaluation of response to shunting in NPH. The current GD method only provides point estimates for each parameter, including R_{out}. Therefore, a patient with R_{out} of 13.0 mmHg/mL/min would be unequivocally assigned to the group above the diagnostic threshold and, using this criterion, would undergo shunt placement surgery. In contrast, consider a scenario whereby the Bayesian approach yielded, for the same patient, R_{out} of 13.5 ± 0.01 mmHg/mL/min compared to 13.5 ± 4.0 mmHg/mL/min. By taking into account the uncertainty, the clinician would be more inclined to categorise the former result in the above-threshold group, and more careful in interpreting the latter. Such nuanced understanding of potentially equivocal results could indicate a need for a repeat test or to give more priority to other clinical variables. Discriminating between these two, vastly different results is crucial in clinical practice, and the new method provides the necessary tools to do so.

The study by Wikkelsø et al. (2013) also raises another point regarding the utility of other CSF dynamics variables, or its lack thereof. In future research, using the Bayesian methodology for the re-evaluation of the relationship between infusion test results and clinical outcome data potentially raises the prospect of utilising other parameters in prognostication of response to shunting. There is a strong case for developing multivariate models that incorporate various diagnostic modalities, including neuroimaging, clinical examination findings, and direct measurements of CSF pressure. Integrating these data sources could significantly enhance diagnostic accuracy for conditions with complex CSF dynamics. To address this need, longitudinal studies should be conducted to assess how accurately this model estimates parameters under various pathological conditions and how these estimations correlate with clinical outcomes, especially in diseases like NPH.

To further advance this approach, enhance its methodological robustness and aid its potential clinical applications, several avenues for future work are proposed. These pertain to the CSF model used and the MCMC approach employed to fit it to data. Although the Marmarou model is the best-known solution for modelling CSF dynamics, it can be criticized as oversimplified. Multiple advancements to this modelling framework have been proposed (Linninger et al., 2016), and incorporating comprehensive physiological data and refining the existing mathematical frameworks may improve the approach described in the current work.

Future investigations could focus on refining the MCMC algorithms by implementing alternative sampling algorithms and exploring the effects of prior distributions on sampling efficiency, convergence, computational cost, and accuracy. For example, Gibbs sampling or the No-U-Turn Sampler (NUTS) can offer alternatives to Metropolis-Hastings approach in the current work. Similarly, moving away from the assumption of normal distribution for priors, other choices such as inverse gamma, half-Cauchy or uniform (non-informative) distributions need to be evaluated.

Through these proposed studies, we aim to not only enhance the computational and analytical capabilities of Bayesian methods in physiological parameter estimation of CSF dynamics parameters but also to bridge the gap between theoretical research and its application in clinical practice.

5. Conclusion

In this study, we have introduced a novel Bayesian approach for the analysis of cerebrospinal fluid (CSF) dynamics in infusion studies, yielding superior goodness of fit and notably reducing erroneous predictions compared to traditional GD methods. This new method yields parameter values aligned with those obtained from extant techniques and uniquely provides posterior distributions for each parameter within individual recordings. This functionality allows a robust quantification of estimation uncertainty, promoting a nuanced and reliable results interpretation. Collectively, our results underscore the Bayesian method's potential to provide accurate, physiologically plausible CSF dynamics estimates, thereby minimizing misdiagnosis or inappropriate treatment risks.

Declaration of competing interest

The authors declare the following financial interests/personal relationships which may be considered as potential competing interests.

Peter Smielewski and Alexis Joannides report financial support and administrative support provided by European Commission: REVERT project (https://revertproject.org) within EC INTERREG program.

Peter Smielewski and Marek Czosnyka report a relationship with Cambridge Enterprise that includes: equity or stocks (part of licensing fees for the ICM+ (https://icmplus.neurosurg.cam.ac.uk)).

Professor Marek Czosnyka is a Guest Editor for The XVIII International Symposium on Intracranial Pressure and Brain Monitoring (ICP 2022)

Erta Beqiri is supported by the Medical Research Council (grant no.: MR N013433-1) and by the Gates Cambridge Scholarship

Acknowledgements

This work was supported by REVERT project (https://revertproject.org) within European Comission INTERREG program. Erta Beqiri is supported by the Medical Research Council (grant no.: MR N013433-1) and by the Gates Cambridge Scholarship.

Appendix

A.1. Model derivation

Mathematical modelling of complex nonlinear systems like CSF dynamics inevitably necessitates simplifications for tractability and comprehensibility. The Marmarou model, with its limited compartments and parameters, may overlook nuanced aspects of CSF physiology, including brain pulsatility effects and the role of the glymphatic system.

This model also operates on several assumptions, such as constant CSF production and a linear pressure-volume relationship. Practically, this implies that even though craniospinal compliance consists of both linear and exponential terms relative to optimal pressure, these are consolidated into a singular lumped elasticity coefficient in the model, simplifying the system's dynamics.

The Marmarou model is mathematically defined by a nonlinear differential equation

$$I_{\mathrm{inf}} = \frac{1}{E \times (P - P_0)} \times \frac{\mathrm{d}p}{\mathrm{d}t} \times \frac{P_{\mathrm{m}} - P_{\mathrm{b}}}{R_{\mathrm{out}}}, \tag{A.1}$$

with the elasticity coefficent E [1/mL] defined as

$$E = \frac{1}{C \times (P_{\mathrm{m}} - P_0)}. \tag{A.2}$$

With

$$I_{\mathrm{f}} = \frac{P_{\mathrm{b}} - P_{\mathrm{ss}}}{R_{\mathrm{out}}}, \tag{A.3}$$

and under the assumption that $P_{\mathrm{ss}} \approx P_0$, this equation has the following analytical solution:

$$\widehat{P}(R_{\mathrm{out}}, E, P_0, t) = \frac{\left(I_{\mathrm{f}} + I_{\mathrm{inf}}\right) \times (P_b - P_0)}{I_{\mathrm{f}} + I_{\mathrm{inf}} \times \exp\left(-Et\left(I_{\mathrm{f}} + I_{\mathrm{inf}}\right)\right)} + I_{\mathrm{inf}}. \tag{A.4}$$

A.2. Metropolis-Hastings algorithm

The CSF dynamics model used to fit the infusion test pressure recordings in this study depends on four parameters: resistance to CSF outflow R_{out}, reference pressure P_0, CSF production rate I_{f}, and brain elasticity coefficient E. Each of these parameters is a physiological value with an established permissible range.

Markov Chain Monte Carlo (MCMC) methods like Metropolis-Hastings are effective in Bayesian inference due to their ability to explore complex posterior distributions and their general insensitivity to prior distributions. They work by creating a Markov chain, iteratively proposing new points based on the current state, which allows them to adapt and converge to the target distribution over time, a concept known as ergodicity.

The algorithm begins with an initial guess for the parameter values, and at each iteration it proposes a new set of values based on a proposal distribution, which is usually taken to be a multivariate Gaussian distribution centred at the current values.

In our study, we assumed Gaussian priors for all parameters, with mean values and standard deviations chosen to reflect the established physiological ranges for each parameter. The likelihood function for the data D given the proposed model parameters θ was given by

$$\mathscr{L}(D|\theta) = \frac{1}{\sqrt{2\pi\sigma^2}} \times \exp\left(-\frac{(D - f(\theta))^2}{2\sigma^2}\right), \tag{A.5}$$

where $f(\theta)$ is the model prediction given the proposed values θ, and σ is the measurement uncertainty.

In the Metropolis-Hastings algorithm, the proposed values are accepted or rejected based on the ratio of the likelihood of the data given the proposed values to the likelihood of the data given the current values, multiplied by the ratio of the proposal distribution evaluated at the current values to the proposal distribution evaluated at the proposed values:

$$\alpha = \frac{\mathscr{L}(D|\theta')}{\mathscr{L}(D|\theta)} \frac{q(\theta|\theta')}{q(\theta'|\theta)} \tag{A.6}$$

where $\mathrm{L}(D\,|\theta)$ is the likelihood of the data D given the proposed values θ, $q(\theta\,|\theta')$ is the proposal distribution evaluated at the current values θ, and $q(\theta'\,|\theta)$ is the proposal distribution evaluated at the proposed values θ'. The parameter values are accepted with probability α, and rejected with probability $1-\alpha$. If the proposed values are accepted, they become the new current values. If they are rejected, the current values remain unchanged. In either case, the new or the old value, is added to the distribution defining set (histogram). This process is repeated for many iterations, with the resulting sequence of accepted values approximating the posterior distribution of the parameters.

Specifically, the algorithm proceeds as follows.

1. Initialize the current values of the parameters, θ, based on the established means.
2. For $t = 1,2, \ldots,T$:
1. Propose a new set of parameter values, θ', from the proposal distribution.

2. Calculate the acceptance ratio
3. Generate a random number $u \sim$ Uniform(0,1).
4. If $u < \alpha$, set $\theta = \theta'$ (accept the proposal). Otherwise, keep θ the same (reject the proposal).

Return the samples $\theta_1, \theta_2, \ldots, \theta_T$ as an estimate of the target distribution.

By running the algorithm for a sufficiently large number of iterations, we can obtain a sample from the posterior distribution of the model parameters, which can be used to estimate the uncertainty in the optimized parameter values.

References

Albeck, M.J., Børgesen, S.E., Gjerris, F., Schmidt, J.F., Sørensen, P.S., 1991. Intracranial pressure and cerebrospinal fluid outflow conductance in healthy subjects. J. Neurosurg. 74 (4), 597–600. https://doi.org/10.3171/jns.1991.74.4.0597.

Albeck, M.J., Skak, C., Nielsen, P.R., Olsen, K.S., Børgesen, S.E., Gjerris, F., 1998. Age dependency of resistance to cerebrospinal fluid outflow. J. Neurosurg. 89 (2), 275–278. https://doi.org/10.3171/jns.1998.89.2.0275.

Andersson, N., Malm, J., Eklund, A., 2008. Dependency of cerebrospinal fluid outflow resistance on intracranial pressure. J. Neurosurg. 109 (5), 918–922. https://doi.org/10.3171/JNS/2008/109/11/0918.

Avezaat, C., van Eijndhoven, J.H.M., 1984. Cerebrospinal Fluid Pulse Pressure and Craniospinal Dynamics: a Theoretical, Clinical and Experimental Study.

Bezanson, J., Edelman, A., Karpinski, S., Julia, V. B. Shah, 2017. A fresh approach to numerical computing. SIAM Rev Soc Ind Appl Math 59 (1), 65–98. https://doi.org/10.1137/141000671.

Cutler, R.W., Page, L., Galicich, J., Watters, G.V., 1968. Formation and absorption of cerebrospinal fluid in man. Brain 91 (4), 707–720. https://doi.org/10.1093/brain/91.4.707.

Czosnyka, M., Wollk-Laniewski, P., Batorski, L., Zaworski, W., 1988. Analysis of intracranial pressure waveform during infusion test. Acta Neurochir. 93, 140–145.

Czosnyka, M., Batorski, L., Laniewski, P., Maksymowicz, W., Koszewski, W., Zaworski, W., 1990. A computer system for the identification of the cerebrospinal compensatory model. Acta Neurochir. 105 (3–4), 112–116. https://doi.org/10.1007/BF01669992.

Czosnyka, M., Czosnyka, Z., Momjian, S., Schmidt, E., 2003. Calculation of the resistance to CSF outflow. J. Neurol. Neurosurg. Psychiatry 74 (9), 1354. https://doi.org/10.1136/jnnp.74.9.1354 author reply 1354–1355.

Czosnyka, Z., Czosnyka, M., Owler, B., Momjian, S., Kasprowicz, M., Schmidt, E.A., Smielewski, P., Pickard, J.D., 2005. Clinical testing of CSF circulation in hydrocephalus. In: Poon, W.S., Chan, M.T.V., Goh, K.Y.C., Lam, J.M.K., Ng, S.C.P., Marmarou, A., Avezaat, C.J.J., Pickard, J.D., Czosnyka, M., Hutchinson, P.J.A., Katayama, Y. (Eds.), Acta Neurochir Suppl. Springer, Vienna, pp. 247–251. https://doi.org/10.1007/3-211-32318-X50. Intracranial Press. Brain Monit. XII.

Czosnyka, Z.H., Czosnyka, M., Smielewski, P., Lalou, A.D., Nabbanja, E., Garnett, M., Barszcz, S., Schmidt, E.A., Momjian, S., Kasprowicz, M., Petrella, G., Owler, B., Keong, N.C., Hutchinson, P.J., Pickard, J.D., 2021. Single center experience in cerebrospinal fluid dynamics testing. In: Pressure, Intracranial, Neuromonitoring, X. V.I.I., Depreitere, B., Meyfroidt, G., Guiza, F. (Eds.), Acta Neurochir Suppl. Springer International Publishing, Cham, pp. 311–313. https://doi.org/10.1007/978-3-030-59436-758.

Deck, M.D., Potts, D.G., 1969. Movements of ventricular fluid levels due to cerebrospinal fluid formation. Am. J. Roentgenol. Radium Ther. Nucl. Med. 106 (2), 354–368. https://doi.org/10.2214/ajr.106.2.354.

Ekstedt, J., 1978. CSF hydrodynamic studies in man. 2 . Normal hydrodynamic variables related to CSF pressure and flow. J. Neurol. Neurosurg. Psychiatry 41 (4), 345–353.

Gelman, A., Rubin, D.B., 1992. Inference from iterative simulation using multiple sequences. Stat. Sci. 457–472.

Gideon, P., Sthlberg, F., Thomsen, C., Gjerris, F., Sørensen, P.S., Henriksen, O., 1994. Cerebrospinal fluid flow and production in patients with normal pressure hydrocephalus studied by MRI. Neuroradiology 36 (3), 210–215. https://doi.org/10.1007/BF00588133.

Hakim, S., Adams, R.D., 1965. The special clinical problem of symptomatic hydrocephalus with normal cerebrospinal fluid pressure. Observations on cerebrospinal fluid hydrodynamics. J. Neurol. Sci. 2 (4), 307–327. https://doi.org/10.1016/0022-510x(65)90016-x.

Hastings, W.K., 1970. Monte Carlo sampling methods using Markov chains and their applications. Biometrika 57 (1), 97–109. https://doi.org/10.2307/2334940.

Hebb, A.O., Cusimano, M.D., 2001. Idiopathic normal pressure hydrocephalus: a systematic review of diagnosis and outcome. Neurosurgery 49 (5), 1166–1184. https://doi.org/10.1097/00006123-200111000-00028 discussion 1184–1186.

Huang, T.-Y., Chung, H.-W., Chen, M.-Y., Giiang, L.-H., Chin, S.-C., Lee, C.-S., Chen, C.-Y., Liu, Y.-J., 2004. Supratentorial cerebrospinal fluid production rate in healthy adults: quantification with two-dimensional cine phase-contrast MR imaging with high temporal and spatial resolution. Radiology 233 (2), 603–608.

Katzman, R., Hussey, F., 1970. A simple constant-infusion manometric test for measurement of CSF absorption. I. Rationale and method. Neurology 20 (6), 534–544. https://doi.org/10.1212/wnl.20.6.534.

Lalou, A.-D., Czosnyka, M., Garnett, M.R., Nabbanja, E., Petrella, G., Hutchinson, P.J., Pickard, J.D., Czosnyka, Z., 2020. Shunt infusion studies: impact on patient outcome, including health economics. Acta Neurochir. 162 (5), 1019–1031. https://doi.org/10.1007/s00701-020-04212-0.

Lalou, A.D., Czosnyka, M., Placek, M.M., Smielewski, P., Nabbanja, E., Czosnyka, Z., 2021. CSF dynamics for shunt prognostication and revision in normal pressure hydrocephalus. J. Clin. Med. 10 (8), 1711. https://doi.org/10.3390/jcm10081711.

Levrini, V., Garnett, M., Nabbanja, E., Czosnyka, M., Czosnyka, Z.H., Lalou, A.D., 2021. Comparison of assessment for shunting with infusion studies versus extended lumbar drainage in suspected normal pressure hydrocephalus. Intracranial Pressure and Neuromonitoring XVII, 355–358.

Linninger, A.A., Tangen, K., Hsu, C.Y., Frim, D., 2016. Cerebrospinal fluid mechanics and its coupling to cerebrovascular dynamics. Annu. Rev. Fluid Mech. 48, 219–257. https://doi.org/10.1146/annurev-fluid-122414-034321.

Lorenzo, A.V., Page, L.K., Watters, G.V., 1970. Relationship between cerebrospinal fluid formation, absorption and pressure in human hydrocephalus. Brain 93 (4), 679–692. https://doi.org/10.1093/brain/93.4.679.

Malm, J., Jacobsson, J., Birgander, R., Eklund, A., 2011. Reference values for CSF outflow resistance and intracranial pressure in healthy elderly. Neurology 76 (10), 903–909. https://doi.org/10.1212/WNL.0b013e31820f2dd0.

Marmarou, A., Shulman, K., LaMorgese, J., 1975. Compartmental analysis of compliance and outflow resistance of the cerebrospinal fluid system. J. Neurosurg. 43 (5), 523–534. https://doi.org/10.3171/jns.1975.43.5.0523.

Masserman, J.H., 1934. Cerebrospinal hydrodynamics: IV. Clinical experimental studies. Arch. Neurol. Psychiatr. 32 (3), 523–553.

Metropolis, N., Rosenbluth, A.W., Rosenbluth, M.N., Teller, A.H., Teller, E., 1953. Equation of state calculations by fast computing machines. J. Chem. Phys. 21 (6), 1087–1092. https://doi.org/10.1063/1.1699114.

Nabbanja, E., Czosnyka, M., Keong, N.C., Garnett, M., Pickard, J.D., Lalou, D.A., Czosnyka, Z., 2018. Is there a link between ICP-derived infusion test parameters and outcome after shunting in normal pressure hydrocephalus? Acta Neurochir. Suppl. 126, 229–232. https://doi.org/10.1007/978-3-319-65798-146.

Okon, M.D., Roberts, C.J., Mahmoud, A.M., Springer, A.N., Small, R.H., McGregor, J.M., Katz, S.E., 2018. Characteristics of the cerebrospinal fluid pressure waveform and craniospinal compliance in idiopathic intracranial hypertension subjects. Fluids Barriers CNS 15 (1), 1–7.

Penn, R.D., Basati, S., Sweetman, B., Guo, X., Linninger, A., 2011. Ventricle wall movements and cerebrospinal fluid flow in hydrocephalus. J. Neurosurg. 115 (1), 159–164. https://doi.org/10.3171/2010.12.JNS10926.

Piechnik, S.K., Summers, P.E., Jezzard, P., Byrne, J.V., 2008. Magnetic resonance measurement of blood and CSF flow rates with phase contrast–normal values, repeatability and CO2 reactivity. Acta Neurochir. Suppl. 102, 263–270. https://doi.org/10.1007/978-3-211-85578-250.

Rottenberg, D.A., Howieson, J., Deck, M.D., 1977. The rate of CSF formation in man: preliminary observations on metrizamide washout as a measure of CSF bulk flow. Ann. Neurol. 2 (6), 503–510. https://doi.org/10.1002/ana.410020610.

Rubin, R.C., Henderson, E.S., Ommaya, A.K., Walker, M.D., Rall, D.P., 1966. The production of cerebrospinal fluid in man and its modification by acetazolamide. J. Neurosurg. 25 (4), 430–436. https://doi.org/10.3171/jns.1966.25.4.0430.

Silverberg, G., Heit, G., Huhn, S., Jaffe, R., Chang, S., Bronte-Stewart, H., Rubenstein, E., Possin, K., Saul, T., 2001. The cerebrospinal fluid production rate is reduced in dementia of the Alzheimer's type. Neurology 57 (10), 1763–1766.

Smielewski, P., Lavinio, A., Timofeev, I., Radolovich, D., Perkes, I., Pickard, J.D., Czosnyka, M., 2009. ICM+, a flexible platform for investigations of cerebrospinal dynamics in clinical practice. In: Steiger, H.J. (Ed.), Acta Neurochir Suppl. Springer, pp. 145–151. https://doi.org/10.1007/978-3-211-85578-230. Acta Neurochir Suppl. Vienna.

Smielewski, P., Czosnyka, Z., Kasprowicz, M., Pickard, J.D., Czosnyka, M., 2012. ICM+: a versatile software for assessment of CSF dynamics. Acta Neurochir. Suppl. 114, 75–79. https://doi.org/10.1007/978-3-7091-0956-413.

Szewczykowski, J., Kunicki, A., Dytko, P., Korsak-liwka, J., et al., 1977. A fast method of estimating the elastance of the intracranial system: a practical application in neurosurgery. J. Neurosurg. 47 (1), 19–26.

Thavarajasingam, S.G., El-Khatib, M., Rea, M., Russo, S., Lemcke, J., Al-Nusair, L., Vajkoczy, P., 2021. Clinical predictors of shunt response in the diagnosis and treatment of idiopathic normal pressure hydrocephalus: a systematic review and meta-analysis. Acta Neurochir. 163 (10), 2641–2672. https://doi.org/10.1007/s00701021-04922-z.

Tisell, M., Edsbagge, M., Stephensen, H., Czosnyka, M., Wikkelsø, C., 2002. Elastance correlates with outcome after endoscopic third ventriculostomy in adults with hydrocephalus caused by primary aqueductal stenosis. Neurosurgery 50 (1), 70–77. https://doi.org/10.1097/00006123-200201000-00013.

Wahlin, A., Ambarki, K., Birgander, R., Alperin, N., Malm, J., Eklund, A., 2010. Assessment of craniospinal pressure-volume indices. Am. J. Neuroradiol. 31 (9), 1645–1650.

Wikkelsø, C., Hellstrom, P., Klinge, P.M., Tans, J.T.J., European iNPH Multi-¨centre Study Group, 2013. The European iNPH multicentre study on the predictive values of resistance to CSF outflow and the CSF tap test in patients with idiopathic normal pressure hydrocephalus. J. Neurol. Neurosurg. Psychiatry 84 (5), 562–568. https://doi.org/10.1136/jnnp-2012-303314.

Yoshida, K., Takahashi, H., Saijo, M., Ueguchi, T., Tanaka, H., Fujita, N., Murase, K., 2009. Phase-contrast MR studies of CSF flow rate in the cerebral aqueduct and cervical subarachnoid space with correlation-based segmentation. Magn. Reson. Med. Sci. 8 (3), 91–100. https://doi.org/10.2463/mrms.8.91.